# Room Temperature Discrimination of Adsorbed Molecules and Attachment Sites on the Si(111)−7 × 7 Surface Using a qPlus Sensor

**Zsolt Majzik,[†] Benedict Drevniok,[‡] Wojciech Kamiński,[§] Martin Ondráček,[†] Alastair B. McLean,[‡,*] and Pavel Jelínek[†,*]**

[†]Institute of Physics, Academy of Sciences of the Czech Republic, Cukrovarnicka 10, 162 53 Prague, Czech Republic, [‡]Department of Physics, Engineering Physics and Astronomy, Queen's University, Kingston, Ontario, Canada K7L 3N6, and [§]Institute of Experimental Physics, University of Wrocław, plac Maksa Borna 9, 50-204 Wrocław, Poland

**ABSTRACT** In this paper, we show that simultaneous noncontact atomic force microscopy (nc-AFM) and scanning tunneling microscopy (STM) is a powerful tool for molecular discrimination on the Si(111)−7 × 7 surface, even at room temperature. Using density functional theory modeling, we justify this approach and show that the force response allows us to distinguish straightforwardly between molecular adsorbates and common defects, such as vacancies. Finally, we prove that STM/nc-AFM method is able to determine attachment sites of molecules deposited on semiconductor surface at room temperature.

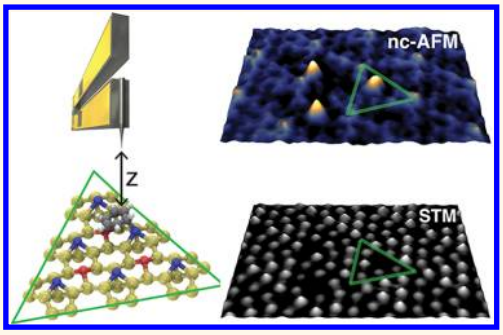


**KEYWORDS:** STM · nc-AFM · Si(111) · benzene · ethylene · chemical identification · molecular recognition

Since crystalline Si is used to manufacture the majority of microelectronic devices, the organic−Si interface has been the subject of intense study, becoming a major focus of nanoscience and technology.[1−6] To manufacture hybrid devices that take advantage of the optical response or the biofunctional properties of organic materials,[7,8] functional molecules must be interfaced to Si in a way that preserves their intrinsic properties.

Although the first atomic-resolution studies of the organic−Si interface formation were performed with scanning tunneling microscopy (STM),[9,10] atomic force microscopy (AFM),[11,12] in particular, noncontact atomic force microscopy (nc-AFM),[13,14] has developed into a powerful probe of molecules on surfaces.[15−18] For example, nc-AFM images of pentacene, collected at liquid helium temperature with a CO-functionalized tip, closely reflect the chemical structure of the pentacene molecule.[17] This capability to sense the atomic structure of molecules has also been used to solve the chemical structure of a molecule.[18]

STM probes the local electronic density of states in the vicinity of the Fermi level, making it a valuable probe of molecular orbitals that frequently extend far beyond the atomic cores.[19,20]

Although these two experimental methods are, in their own right, powerful probes of molecules on surfaces, the measurements can be performed concurrently.[21−28] With the development of self-sensing sensors, such as the qPlus,[29] that do not require a laser to measure the deflection, it has become simple to combine these two techniques. In the qPlus configuration, the microfabricated silicon cantilevers are replaced by stiff, piezoelectric quartz tuning forks similar to those used as frequency etalons in watches. The qPlus methodology offers several advantages besides simplicity; quartz has the optimal stiffness for low amplitude operation that is essential for improving the sensitivity of short-range interactions, and the tunneling current can appear over a larger portion of an oscillation cycle, leading to its improved detection.

* Address correspondence to mclean@physics.queensu.ca, jelinekp@fzu.cz.

Received for review January 8, 2013 and accepted February 22, 2013.

**Published online** 10.1021/nn400102m

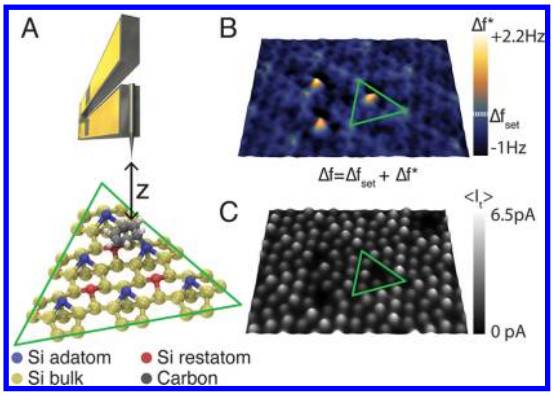


**Figure 1. (A) Schematic representation of a qPlus sensor (not to scale) that is used to simultaneously measure the time-averaged tunneling current $\langle I_t \rangle$ and the frequency shift $\Delta f$ caused by tip−surface interaction. The bias voltage was set to +0.05 V and the $\Delta f$ set point to −9 Hz. The amplitude (0.24 nm) of the *z* motion has been drawn to scale with the atomic model that shows half of the Si(111)−7 × 7 unit cell and a single benzene adsorbate. (B) nc-AFM ($\Delta f$) image of the Si(111)−7 × 7 surface clearly showing (bright spots) three benzene adsorbates. (C) Simultaneously acquired STM ($\langle I_t \rangle$) image. The chemisorbed benzene molecule results in a darkened Si adatom, similar to a vacancy, and cannot be easily identified in $\langle I_t \rangle$ images. Green triangles in (B) and (C) denote the Si(111)−7 × 7 half unit cell containing a benzene molecule.**

In this paper, we use a qPlus sensor to study ethylene, benzene, and hydrogen adsorbates on the reactive Si(111)−7 × 7 surface, using simultaneous STM/nc-AFM at room temperature (see Figure 1). These systems have been studied before, and they can be considered to be model systems.[30−40] Using STM alone, it is hard to distinguish adsorbates from Si adatom vacancies, a common defect on this surface, because the bond formation with a Si adatom, the most reactive surface site for nucleophilic adsorbates,[41] also lowers the density of states in the vicinity of the Fermi level.[9,10,40] We demonstrate a straightforward way to distinguish adsorbates like benzene and ethylene from Si adatom vacancies, using the simultaneous acquisition of frequency shift $\Delta f$ and time-averaged tunneling current $\langle I_t \rangle$ images. We will also demonstrate that the $\Delta f$ signal, for the specific cases of Si(111)−7 × 7/benzene and ethylene, provides very detailed information about the attachment geometry. The additional information provided by the simultaneous STM/nc-AFM measurement will allow more accurate modeling of molecular self-organization on reactive surfaces like Si(111)−7 × 7 than has been possible to date.[42−44] These findings have important implications for the molecular-level design of organic and molecular-electronic devices.

## RESULTS AND DISCUSSION

**Discriminating Ethylene from Si Adatom Vacancies.** Constant-current STM images of the clean Si(111)−7 × 7 surface, and of the same surface after ethylene exposure, are presented in Figure 2. The clean surface

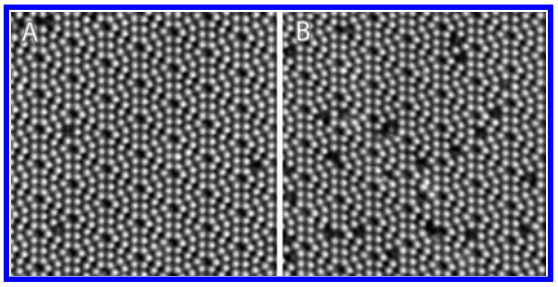


**Figure 2. (A) Constant-current STM topography of the Si(111)−7 × 7 surface immediately after cleaning in UHV; the dominant surface defect is the Si adatom vacancy. (B) After adsorbing 50 L of ethylene, the number of darkened adatoms increases. The size of images is 24.5 nm × 24.5 nm. They were collected with a sample bias of +1.0 V and a current set point of 0.1 nA.**

(panel A) contains a low areal density of Si adatom vacancies, the most common defect on the clean surface. After exposure to ethylene, for reasons presented above, the density of darkened Si adatoms increases (panel B). A surface cleaned in UHV and exposed to benzene has a similar appearance.[32,45,46] For what will come below, it is important to appreciate that although both benzene and ethylene form a di-$\sigma$ bond with the surface, bridging a Si adatom and a Si restatom, in the STM constant-current image, only the Si adatom is darkened. Consequently, if the molecule forms a bond with the edge adatom, it is not straightforward to identify which restatom is involved. There are two nearest-neighbor restatoms for every Si edge adatom. This is a limitation of the STM constant-current imaging modality that will be discussed later. Moreover, to distinguish an adsorbed molecule from a Si vacancy using STM, a high bias voltage must be used. Unfortunately, the high local electric field produced by the high bias voltage leads to unstable imaging conditions and the increased risk of the manipulation of surface species.

To understand the atomic contrast observed with nc-AFM, let us first discuss site-specific force spectroscopy measurements on the Si(111)−7 × 7 surface after exposure to ethylene. Force-site spectroscopy was performed over Si adatoms, ethylene adsorption sites, and adatom vacancies. Figure 3A contains the short-range force curves that were measured above different sites on an ethylene-exposed Si(111)−7 × 7 surface. The force is zero far from the surface. As the tip is moved toward a Si adatom, the probe experiences an attractive force due to the formation of the chemical bond between the frontier atoms of the tip and the sample. When the tip further approaches the surface (not shown), the short-range force reverses sign and becomes repulsive, as expected.[47] Over the ethylene adsorption site, the behavior is different. As the tip is moved toward the ethylene molecule, there is a very small attractive force. However, the short-range force then changes sign and becomes repulsive due to Pauli

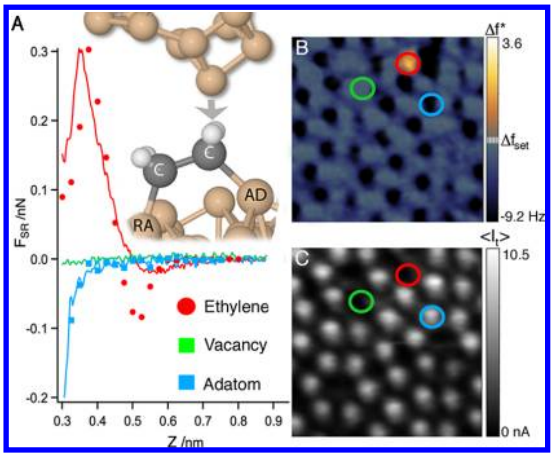


**Figure 3. (A) Measured (lines) and calculated (points) force−distance curves for ethylene, a Si adatom, and an adatom vacancy on Si(111)−7 × 7 with *z* being the tip height. Only short-range forces ($F_{SR}$) are presented (see Methods). The $\Delta f$ image (5 nm × 5 nm) is presented in panel B. The constant-height scanning was performed with a slow $\Delta f$ feedback set to −6 Hz. The oscillation amplitude was 0.13 nm. The bias voltage was tuned to the contact potential difference (CPD) minimum, which we found to be +0.4 V. (C) Constant-height $\langle I_t \rangle$ image that was acquired simultaneously with (B) after the Si(111)−7 × 7 surface had been exposed to 50 L of ethylene. A silicon adatom is identified with a blue circle, the ethylene molecule with a red circle, and the Si adatom vacancy with a green circle.**

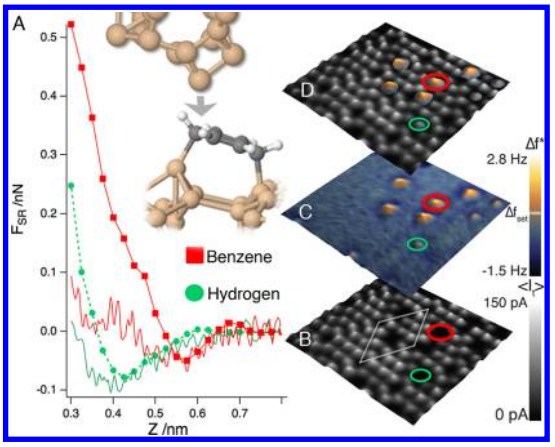


**Figure 4. (A) Force-site spectroscopy measured (continuous lines) and calculated (points) over a hydrogen atom and a benzene molecule on a Si(111)−7 × 7 surface that had been exposed to 50 L of benzene. Only short-range forces ($F_{SR}$) are presented (see Methods). (B) STM image ($\langle I_t \rangle$) of 10 nm × 8 nm, measured in constant-height mode, and (C) $\Delta f$ (nc-AFM) image acquired simultaneously. (D) Overlay image generated by superimposing the two. The constant-height scanning was performed with a slow $\Delta f$ feedback set to −7.1 Hz. The oscillation amplitude was 0.24 nm. The bias voltage was set to the CPD minimum at 0.4 V. In (B), the white lines delineate a unit cell of the 7 × 7 surface reconstruction. The red and blue circles are used to identify hydrogen and benzene adsorbates, respectively.**

repulsion at closer distances. Comparing both force curves taken over the molecule and the adatom site, we found that the onset of the repulsive force occurs further from the surface for the ethylene site, a reflection of the fact that the molecule is further from the surface. Finally, within the tip−sample separation that we explored, we were not able to detect any short-range force over a vacancy.

We performed density functional theory (DFT) simulations where a Si-based tip was approached over a Si adatom, a Si vacancy, and an ethylene molecule adsorbed on the Si(111)−7 × 7 surface (see Figure 3A). Our calculated force spectra show very similar tendencies to our experimental measurements. There is only a small discrepancy on the maximal attractive force over the ethylene molecule, which we attribute to the approximations used in our calculations (*i.e.*, the LDA functional and the local basis set or the tip model). It can be noticed that both experimental and theoretical force curves show decreased repulsive interaction when the tip−sample separation is below 0.4 nm. From our DFT simulations, we relate this effect to a downward bending of the H atom, due to the Pauli repulsion.

From the discussion presented above, it is evident that the force response allows us to discriminate different species on the surface. If a scan is performed in constant-height mode, with the tip−sample distance adjusted to the onset of the repulsive force over the molecular site, each species will provide a characteristic short-range force interaction. Specifically, the Si adatom induces an attractive force, the ethylene molecule induces a repulsive force, and there is no detectable short-range interaction for the Si adatom vacancy.

To demonstrate the efficacy of using the force interaction to discriminate surface species, we collected combined STM/nc-AFM images from ethylene-exposed Si(111)−7 × 7 surfaces. Images derived from the frequency shift $\Delta f$ and the average tunneling current $\langle I_t \rangle$ of the ethylene-exposed surface are shown in Figure 3B,C. The STM image contains two darkened Si adatoms (red and green circles in Figure 3C). The dark spots in the $\Delta f$ image are generated by a net attractive force, and they are coincident with the known positions of the Si adatoms from the $\langle I_t \rangle$ channel. The atomic positions derived from the STM image have been added to the nc-AFM image in Figure 3B. A bright protrusion (red circle in B), caused by a net repulsive force, can be seen near one missing adatom that is located at the edge of the half unit cell. On the basis of the discussion above, this is the characteristic behavior of an adsorbed ethylene molecule. Contrastingly, we recorded no short-range interaction over another darkened adatom site (green circle in Figure 3C), and therefore, this site is an adatom vacancy.

**Discriminating Benzene from Hydrogen.** To further demonstrate the robustness of this methodology, we also performed measurements on a Si(111)−7 × 7 surface with adsorbed benzene and atomic hydrogen. Resulting images of $\langle I_t \rangle$ and $\Delta f$, collected at constant height and presented in Figure 4, are similar to those presented earlier for ethylene. However, the presence of

two different adsorbates gives rise to two different signatures. The constant-height STM/nc-AFM images (Figure 4B–D) sample a region of the surface that also contains atomic hydrogen adsorbates. As mentioned above, using only STM, it is difficult to distinguish hydrogen or benzene from native Si vacancies at low bias voltages because the adsorption of both hydrogen and benzene lowers the density of states near the Fermi level. In contrast, both hydrogen and benzene can be readily distinguished from vacancies in the $\Delta f$ image due to the presence of a net repulsive force over the molecules. Note that the $\Delta f$ images were taken sufficiently far from the surface so that Si adatoms are not seen, due to the lack of an attractive short-range force. Nevertheless, the location of the $7 \times 7$ lattice can be detected using the STM channel. From this example, it is evident that the combination of simultaneously recorded nc-AFM and STM channels provides more comprehensive information about surface species on Si(111)–$7 \times 7$.

We can discriminate hydrogen from benzene because the hydrogen force curve is different from the benzene force curve (Figure 4A); the maximum attractive force for the hydrogen site is displaced by more than 0.1 nm from the maximum attractive force for the benzene site (Figure 4A). Also, the bright spots are smaller for hydrogen (Figure 4C), indicating that the net repulsive interaction is smaller, too.

The arguments presented above are based upon our measured force curves. To find further support for the method we have used to discriminate species on the $7 \times 7$ surface reconstruction, we carried out DFT simulations of force spectra over benzene and hydrogen adsorbates. The comparison between experimental and theoretical force–distance curves (see Figure 4A) fully supports our experimental approach. When compared to benzene, the hydrogen atom gives slightly larger maximal attractive short-range force located $\approx$0.15 nm toward the surface. The disagreement between theory and experiment is only seen at very close distances and might be due to the limited size of our tip models, which cannot correctly describe the mechanical response under large load. A more detailed discussion of this effect can be found elsewhere.[48]

**Identification of Attachment Sites.** Next, we demonstrate that combined STM/nc-AFM measurements allow us not only to discriminate different species on the surface (molecule, vacancy, or atomic hydrogen) but also to determine the attachment configuration of a molecule. Ethylene[33,39,40] and benzene[30,32–38,45] both form a di-$\sigma$ covalent bond with the Si(111)–$7 \times 7$ surface at room temperature, bridging a Si adatom and a Si restatom. Although it is possible to image adsorbed molecules with nc-AFM, resolving both the molecule and the Si surface is a more challenging task. To resolve the Si adatoms, the tip would have to be moved close to the surface, but then the probe will experience large repulsive forces over the adsorbate site. Especially at room temperature, these forces lead to tip instabilities during scanning. Consequently, to ensure stable imaging conditions at room temperature, the probe should be scanned in constant-height mode far from the surface.

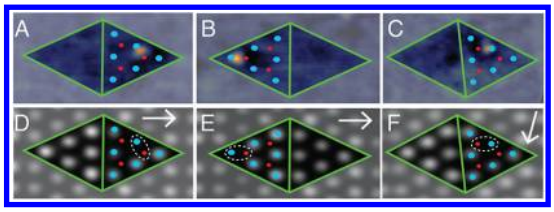


**Figure 5. Top panels: $\Delta f$ images from benzene adsorbates located in (A) edge, (B) corner, and (C) edge sites. In these sites, the molecules bridge edge or corner Si adatoms and the restatoms identified in the bottom panels. Bottom panels (D–F): concurrently acquired $\langle I_t \rangle$ images from the same areas. Panel A was acquired at the same time as panel D and likewise for B and E, and C and F. The fast scan direction is indicated using an arrow; the adsorbate signatures are not influenced by the scan direction. The green lines identify the $7 \times 7$ half unit cell which has a side of length 2.7 nm. All images are recorded at a bias voltage of +0.05 V, and $\Delta f$ set point of −30 Hz. The oscillation amplitude was 0.24 nm.**

With a constant-height scan, the average tunneling current $\langle I_t \rangle$ can be used to identify atomic positions on the surface, while the frequency shift $\Delta f$ can be used to detect molecules. This circumvents the need to move the tip close to the surface to detect the Si adatoms.

Figure 5 shows the results of several STM/nc-AFM measurements taken over a Si(111)–$7 \times 7$ surface that had been exposed to benzene. The molecule produces a strong repulsive interaction with the tip (see top panels of Figure 5), while the adatom, as discussed previously, is missing in the STM channel (see bottom panels of Figure 5). Due to the fact that the constant-height set point is set so far from the surface, the Si adatoms are not resolved in the $\Delta f$ channel. If the STM channel is used to locate the Si adatoms that do not form bonds with a benzene molecule, then it is clear that the repulsive peaks are systematically displaced away from the Si adatom, toward the nearest Si restatom. The displacement does not depend on the scan direction. From this displacement, the Si adatom and the Si restatom that form covalent bonds with the adsorbate can be identified. We observed a similar displacement toward the restatom for ethylene. However, no displacement is observed for hydrogen, as expected.

Consequently, on Si(111)–$7 \times 7$, adsorption sites can be identified with STM/nc-AFM. The location of the $7 \times 7$ lattice is established with STM. The location of the adsorbate, within the $7 \times 7$ cell, is determined using the repulsive interaction detected with nc-AFM. Using STM alone, it would be necessary to scan with high bias voltages to distinguish adsorbed hydrogen

from adsorbed ethylene or benzene, increasing, because of the high local electric field, the risk of manipulation.

Using a constant-height nc-AFM scan, it would not be possible to determine the registry of the molecule relative to the surface because the tip would have to be withdrawn far from the surface to reduce the chance of tip changes. The combined STM/nc-AFM approach reduces the risk of manipulation caused by tip−sample interaction during nc-AFM scanning because the position of the Si adatoms is visible in the $\langle I_t \rangle$ images even when the tip is pulled back from the surface.

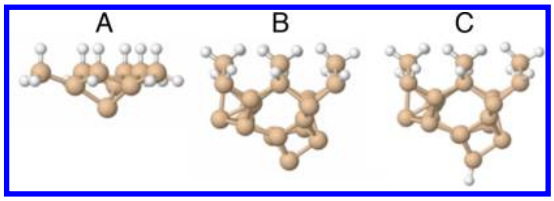


**Figure 6. Ball-and-stick models of the AFM tips considered in simulations: (A) Si tip based on the restatom configuration of the Si(111)−7 × 7 surface (10 Si and 15 H atoms saturating the tip base); (B) dimer-like tip termination similar to the dimer structure of the reconstructed Si(100) surface (30 Si and 18 H atoms); finally, (C) H-terminated dimer-like tip (30 Si and 19 H atoms).**

## CONCLUSIONS

We have shown that the STM/nc-AFM technique complemented with DFT modeling is a powerful tool for discriminating molecules and identifying attachment sites on the semiconductor surface at room temperature, while preserving stable imaging conditions for both the molecule and surface atoms and minimizing the likelihood of tip changes. This approach has considerable promise for discriminating different species of adsorbed molecules on Si(111)−7 × 7 surfaces, including atomic hydrogen. It also reduces the risk of manipulation caused by tip−sample interaction during nc-AFM scanning because the position of the Si adatoms is visible in the $\langle I_t \rangle$ images even when the tip is pulled back from the surface. We believe that the approach that we have described in this paper can be extended to other surfaces, including, specifically, the class of semiconductor surface reconstructions that contain dangling bonds.

## METHODS

**Combined STM/nc-AFM.** The STM/nc-AFM measurements were performed with an Omicron VT XA qPlus AFM/STM system operating with a base pressure below $1 \times 10^{-10}$ mbar with the sample at room temperature. A Specs-Nanonis OC4 was used for the FM demodulation and the Omicron MATRIX control system for the data acquisition. The qPlus sensors were built from tuning forks manufactured by Micro Crystal (MS1V-T1K). Chemically etched tungsten tips were mounted at the end of the free prong. In order to eliminate the so-called cross-talk phenomenon, the internal wiring of the microscope was changed as we have described elsewhere.[49]

Site-specific force spectroscopy was performed by recording the frequency shift from the resonance frequency ($\Delta f$) induced by tip−sample interaction forces while gradually changing the tip−sample separation ($z$). The interaction force between the tip and surface atoms was calculated from the measured $\Delta f$ data using the Sader formula.[50] To be able to disentangle the long-range and short-range force components, we perform the site-specific force spectroscopy above given bright and/or occluded Si adatom site and complementary measurement above a corner hole. The short-range force above each site is obtained as a difference between these two $F(z)$ curves. We aligned $Z$-distance in all figures showing spectroscopy data to distances corresponding to theoretical calculations.

The tunneling current $I_t$ was calculated from time-averaged tunneling current $\langle I_t \rangle$ using a similar approach.[51] For these calculations, the stiffness of the sensor was obtained from FFT analyses of the thermal motion of the lever at room temperature.[52]

Ethylene (Linde, Germany) and benzene (Sigma-Aldrich) were both dosed using a precision leak valve, whereas the atomic hydrogen was deposited by using a commercial source manufactured by FOCUS. All measurements presented were done at room temperature (≈300 K). The purity of the adsorbants was monitored by a quadrupole mass spectrometer (Balzers-Pfeiffer).

**Theoretical nc-AFM Simulations: Methodology and Computational Details.** We performed first-principles calculations based on density functional theory (DFT) with a local-orbital basis using the Fireball code.[53,54] Given the size of 7 × 7 surface unit cell, this is a method of choice due to a favorable accuracy-to-efficiency balance. The calculations were performed within the local-density approximation (LDA) for the exchange-correlation functional.[55] The valence electrons have been described by optimized[56] numerical atomic-like orbitals having the following cutoff radii (all in au): $R_C(s) = 3.8$, and $R_C(s^*) = 3.8$ for H orbitals; $R_C(s) = 4.0$, $R_C(p) = 4.5$, and $R_C(d) = 5.4$ for C orbitals; and $R_C(s) = 4.8$, $R_C(p) = 5.4$, and $R_C(d) = 5.6$ for Si orbitals.

*Ethylene/Benzene Adsorption on Si(111)−7 × 7.* The Si(111) surface was modeled in a 7 × 7 supercell geometry, using a slab of six Si atomic layers, with the bottom side of the slab passivated with H atoms, so the total number of atoms in the supercell was 347. The Si equilibrium bulk lattice parameter of 5.46 Å was used to create the slab geometry. The five top Si layers of the slab were allowed to relax during the optimization process, whereas the rest of the atoms were kept fixed in their initial positions. The equilibrium adsorption geometry of ethylene/benzene on the Si(111)−7 × 7 surface was sought among different adsorption sites and configurations, including dehydrogenation of molecules. All electronic and structural optimizations have been performed until the convergence criteria of $10^{-6}$ eV for the accuracy of the total energy and 0.05 eV/Å for the maximum force acting on the relaxed atoms were satisfied. The structural simulations were carried out using only the Γ-point.

*nc-AFM Simulations.* For the ground-state ethylene/benzene-on-silicon configurations, we have performed a quasi-static approach force *versus* distance calculations (*i.e.*, at 0 K) using three distinct silicon tips[48] (see Figure 6). We have to mention that phenyl- or vinyl-terminated tips may form under certain conditions, and they need to be considered if commonly used tip models do not give reasonable agreements. The theoretical force−distance curves presented in this paper are calculated with the dimer-like tip (see Figure 6B), which provides the best agreement with experiment. In our simulations the tip was gradually moved toward the surface in steps of 0.25 Å along the surface normal. At every such step, all of atoms of the molecule/Si(111) sample and the AFM tip (except for the bottom layer of the slab and the base part of the tip) were allowed to relax to their ground-state configuration, fulfilling the convergence criteria specified above. The total short-range tip−sample forces were then determined as a sum of the final forces acting on the fixed atoms of the tip. This tip approach

procedure was applied for a few specific sites over the adsorbed ethylene/benzene molecules, on top of adatom of clean Si(111), above surface vacancy (missing adatom), and on top of adsorbed atomic H. The 5 Å range of tip−sample distances covers both atractive and repulsive regions, which is important for further molecular discrimination. $Z = 0$ corresponds to the situation where both outermost tip-apex atom and Si layer (*i.e.*, Si adatoms) would have the same *z*-coordinate without any relaxation. This approach has already been successfully employed in a number of previous theoretical studies of the FM-AFM operation (see ref 57 and references therein).

*Conflict of Interest:* The authors declare no competing financial interest.

*Acknowledgment.* We acknowledge financial support from Grant No. GAAV M100101207, GACR, Project No. 204/10/0952, and the Natural Sciences and Engineering Research Council of Canada (NSERC). W.K. thanks the Project No. 1010/S/IFD for support. M.O. acknowledges support from Project No. P204/11/P578 of the Czech Science Foundation (GAČR).

## REFERENCES AND NOTES

1. Buriak, J. M. Organometallic Chemistry on Silicon and Germanium Surfaces. *Chem. Rev.* **2002**, *102*, 1271–1308.
2. Bent, S. F. Organic Functionalization of Group IV Semiconductor Surfaces: Principles, Examples, Applications, and Prospects. *Surf. Sci.* **2002**, *500*, 879–903.
3. Filler, M. A.; Bent, S. F. The Surface as Molecular Reagent: Organic Chemistry at the Semiconductor Interface. *Prog. Surf. Sci.* **2003**, *73*, 1–56.
4. McNab, I. R.; Polanyi, J. C. Patterned Atomic Reaction at Surfaces. *Chem. Rev.* **2006**, *106*, 4321–4354.
5. Leftwich, T. R.; Teplyakov, A. V. Chemical Manipulation of Multifunctional Hydrocarbons on Silicon Surfaces. *Surf. Sci. Rep.* **2008**, *63*, 1–71.
6. Hamers, R. Formation and Characterization of Organic Monolayers on Semiconductor Surfaces. *Annu. Rev. Anal. Chem.* **2008**, *1*, 707–736.
7. Heath, J. Molecular Electronics. *Annu. Rev. Mater. Res.* **2009**, *39*, 1–23.
8. Vilan, A.; Yaffe, O.; Biller, A.; Salomon, A.; Kahn, A.; Cahen, D. Molecules on Si: Electronics with Chemistry. *Adv. Mater.* **2010**, *22*, 140–159.
9. Avouris, P.; Wolkow, R. Atom-Resolved Surface Chemistry Studied by Scanning Tunneling Microscopy and Spectroscopy. *Phys. Rev. B* **1989**, *39*, 5091–5100.
10. Avouris, P. Atom-Resolved Surface Chemistry Using the Scanning Tunneling Microscope. *J. Phys. Chem.* **1990**, *94*, 2246–2256.
11. Binnig, G.; Quate, C.; Gerber, C. Atomic Force Microscope. *Phys. Rev. Lett.* **1986**, *56*, 930–933.
12. Binnig, G.; Gerber, C.; Stoll, E.; Albrecht, T. R.; Quate, C. F. Atomic Resolution with Atomic Force Microscope. *Surf. Sci.* **1987**, *189−190*, 1–6.
13. Albrecht, T.; Quate, C. Atomic Resolution Imaging of a Nonconductor by Atomic Force Microscopy. *J. Appl. Phys.* **1987**, *62*, 2599–2602.
14. Giessibl, F. Atomic Resolution of the Si(111)−7×7 Surface by Atomic Force Microscopy. *Science* **1995**, *267*, 68–71.
15. Morita, S.; Wiesendanger, R.; Meyer, E. *Noncontact Atomic Force Microscopy*; Springer: Berlin, 2002; Vol. 1.
16. Morita, S.; Giessibl, F. J.; Wiesendanger, R. *Atomic Force Microscopy*; Springer: Berlin, 2009; Vol. 2.
17. Gross, L.; Mohn, F.; Moll, N.; Liljeroth, P.; Meyer, G. The Chemical Structure of a Molecule Resolved by Atomic Force Microscopy. *Science* **2009**, *325*, 1110–1114.
18. Gross, L.; Mohn, F.; Moll, N.; Meyer, G.; Ebel, R.; Abdel-Mageed, W. M.; Jaspars, M. Organic Structure Determination Using Atomic-Resolution Scanning Probe Microscopy. *Nat. Chem.* **2010**, *2*, 821–825.
19. Repp, J.; Meyer, G.; Stojkovic, S.; Gourdon, A.; Joachim, C. Molecules on Insulating Films: Scanning-Tunneling Microscopy Imaging of Individual Molecular Orbitals. *Phys. Rev. Lett.* **2005**, *94*, 026803.
20. Wu, S.; Ogawa, N.; Ho, W. Atomic-Scale Coupling of Photons to Single-Molecule Junctions. *Science* **2006**, *312*, 1362–1365.
21. Dürig, U.; Gimzewski, J. K.; Pohl, D. W. Experimental Observation of Forces Acting during Scanning Tunneling Microscopy. *Phys. Rev. Lett.* **1986**, *57*, 2403–2406.
22. Schirmeisen, A.; Cross, G.; Stalder, A.; Grutter, P.; Dürig, U. Metallic Adhesion and Tunnelling at the Atomic Scale. *New J. Phys.* **2000**, *2*, 29.
23. Loppacher, C.; Bammerlin, M.; Guggisberg, M.; Schär, S.; Bennewitz, R.; Baratoff, A.; Meyer, E.; Güntherodt, H. J. Dynamic Force Microscopy of Copper Surfaces: Atomic Resolution and Distance Dependence of Dip−Sample Interaction and Tunneling Current. *Phys. Rev. B* **2000**, *62*, 16944–16949.
24. Hembacher, S.; Giessibl, F.; Mannhart, J.; Quate, C. Revealing the Hidden Atom in Graphite by Low-Temperature Atomic Force Microscopy. *Proc. Natl. Acad. Sci. U.S.A.* **2003**, *100*, 12539–12542.
25. Sawada, D.; Sugimoto, Y.; Morita, K.-i.; Abe, M.; Morita, S. Simultaneous Measurement of Force and Tunneling Current at Room Temperature. *Appl. Phys. Lett.* **2009**, *94*, 173117.
26. Sugimoto, Y.; Yi, I.; Morita, K.-i.; Abe, M.; Morita, S. Simultaneous Force and Current Mapping of the Si(111)−7×7 Surface by Dynamic Force Microscopy. *Appl. Phys. Lett.* **2010**, *96*, 263114.
27. Sugimoto, Y.; Nakajima, Y.; Sawada, D.; Morita, K.-i.; Abe, M.; Morita, S. Simultaneous AFM and STM Measurements on the Si(111)−7×7 Surface. *Phys. Rev. B* **2010**, *81*, 245322.
28. Setvin, M.; Mutombo, P.; Ondracek, M.; Majzik, Z.; Svec, M.; Chab, V.; Ostadal, I.; Sobotik, P.; Jelinek, P. Chemical Identification of Single Atoms in Heterogeneous III−IV Chains on Si(100) Surface by Means of nc-AFM and DFT Calculations. *ACS Nano* **2012**, *6*, 6969–6976.
29. Giessibl, F. Atomic Resolution on Si(111)−7×7 by Non-Contact Atomic Force Microscopy with a Force Sensor Based on a Quartz Tuning Fork. *Appl. Phys. Lett.* **2000**, *76*, 1470–1472.
30. Carbone, M.; Piancastelli, M. N.; Casaletto, M. P.; Zanoni, R.; Comtet, G.; Dujardin, G.; Hellner, L. Low-Temperature Adsorption States of Benzene on Si(111)−7×7 Studied by Synchrotron-Radiation Photoemission. *Phys. Rev. B* **2000**, *61*, 8531–8536.
31. Wang, Z.; Cao, Y.; Xu, G. The Binding of Benzene on Si(111)−7×7: A Theoretical Modelling Approach. *Chem. Phys. Lett.* **2001**, *338*, 7–13.
32. Kawasaki, T.; Sakai, D.; Kishimoto, H.; Akbar, A.; Ogawa, T.; Oshima, C. Adsorption and Desorption of Benzene on Si(111)−7×7 Studied by Scanning Tunnelling Microscopy. *Surf. Interface Anal.* **2001**, *31*, 126–130.
33. Lu, X.; Wang, X.; Yuan, Q.; Zhang, Q. Diradical Mechanisms for the Cycloaddition Reactions of 1,3-Butadiene, Benzene, Thiophene, Ethylene and Acetylene on a Si(111)−7×7. *J. Am. Chem. Soc.* **2003**, *125*, 7923–7929.
34. Petsalakis, I.; Polanyi, J.; Theodorakopoulos, G. Theoretical Study of the Induced Attachment of Benzene to Si(111)−7×7. *Surf. Sci.* **2003**, *544*, 162–169.
35. Tomimoto, H.; Sekitani, T.; Sumii, R.; Oda Sako, E.; Wada, S.; Tanaka, K. Study of Adsorption Structure of Benzene and Toluene on Si(111)−7×7 Surfaces. *Surf. Sci.* **2004**, *566-568*, 664–670.
36. Petsalakis, I.; Polanyi, J. Theoretical Study of Benzene, Toluene, and Dibromobenzene at a Si(111)−7×7 Surface. *Isr. J. Chem.* **2005**, *45*, 111–126.
37. Yong, K.; Yang, S.; Zhang, Y.; Wu, P.; Xu, G. Adsorption-Induced Desorption of Benzene on Si(111)−7×7 by Substrate-Mediated Electronic Interactions. *Langmuir* **2008**, *24*, 3289–3293.
38. Horn, S. A.; Patitsas, S. N. STM Study of Charge Transfer and the Role of Rest-Atoms in the Binding of Benzene to Si(111)−7×7. *Surf. Sci.* **2008**, *602*, 630–637.
39. Yang, F.; Hunger, R.; Roodenko, K.; Hinrichs, K.; Rademann, K.; Rappich, J. Vibrational and Electronic Characterization of Ethynyl Derivatives Grafted onto Hydrogenated Si(111) Surfaces. *Langmuir* **2009**, *25*, 9313–9318.

40. Majzik, Z.; Kamiński, W.; Weymouth, A. J.; Vondráček, M.; Zobač, V.; Švec, M.; Berkó, A.; McLean, A.; Prince, K. C.; Jelinek, P.; *et al.* An Investigation of Ethylene Attachment to Si(111)−7×7 in the Restatom−Adatom Bridging Geometry: Electronic and Vibrational Properties. *J. Phys. Chem. C* **2011**, *115*, 21791–21799.
41. Brommer, K.; Galván, M.; Dal Pino, A.; Joannopoulos, J. Theory of Adsorption of Atoms and Molecules on Si(111)−7×7. *Surf. Sci.* **1994**, *314*, 57–70.
42. Weymouth, A. J.; Miwa, R. H.; Srivastava, G. P.; McLean, A. B. The Role of a Precursor State in Thiophene Chemisorption on Si(111)−7×7. *Phys. Status Solidi C* **2010**, *7*, 240–243.
43. Weymouth, A.; Edge, G.; McLean, A.; Miwa, R.; Srivastava, G. Templating an Organic Layer with the Si(111)−7×7 Surface Reconstruction Using Steric Constraints. *Phys. Rev. B* **2011**, *84*, 165308.
44. Weymouth, A. J.; Miwa, R. H.; Edge, G. J. A.; Srivastava, G. P.; McLean, A. B. Templating an Organic Array with Si(111)−7×7. *Chem. Commun.* **2011**, *47*, 8031–8033.
45. Wolkow, R.; Moffatt, D. The Frustrated Motion of Benzene on the Surface of Si(111). *J. Chem. Phys.* **1995**, *103*, 10696–10700.
46. Brown, D.; Moffatt, D.; Wolkow, R. Isolation of an Intrinsic Precursor to Molecular Chemisorption. *Science* **1998**, *279*, 542–544.
47. Lantz, M. A.; Hug, H. J.; Hoffmann, R.; van Schendel, P. J. A.; Kappenberger, P.; Martin, S.; Baratoff, A.; Guntherodt, H. J. Quantitative Measurement of Short-Range Chemical Bonding Forces. *Science* **2001**, *291*, 2580–2583.
48. Pou, P.; Ghasemi, S. A.; Jelínek, P.; Lenosky, T.; Goedecker, S.; Pérez, R. Structure and Stability of Semiconductor Tip Apexes for Atomic Force Microscopy. *Nanotechnology* **2009**, *26*, 264015.
49. Majzik, Z.; Setvin, M.; Bettac, A.; Feltz, A.; Cháb, V.; Jelinek, P. Simultaneous Current, Force and Dissipation Measurements on the Si(111)−7×7 Surface with an Optimized qPlus AFM/STM Technique. *Beilstein J. Nanotechnol.* **2012**, *3*, 249–259.
50. Sader, J.; Jarvis, S. Accurate Formulas for Interaction Force and Energy in Frequency Modulation Force Spectroscopy. *Appl. Phys. Lett.* **2004**, *84*, 1801–1803.
51. Sader, J. E.; Sugimoto, Y. Accurate Formula for Conversion of Tunneling Current in Dynamic Atomic Force Spectroscopy. *Appl. Phys. Lett.* **2010**, *97*, 043502.
52. Berger, J.; Švec, M.; Müller, M.; Ledinský, M.; Fejfar, A.; Jelínek, P.; Majzik, Z. Characterization of the Mechanical Properties of qPlus Sensors. *Beilstein J. Nanotechnol.* **2013**, *4*, 1–9.
53. Lewis, J. P.; Glaesemann, K. R.; Voth, G. A.; Fritsch, J.; Demkov, A. A.; Ortega, J.; Sankey, O. F. Further Developments in the Local-Orbital Density-Functional-Theory Tight-Binding Method. *Phys. Rev. B* **2001**, *64*, 195103.
54. Jelínek, P.; Wang, H.; Lewis, J. P.; Sankey, O. F.; Ortega, J. Approach to the Exchange-Correlation Interactions in *Ab Initio* Tight-Binding Methods. *Phys. Rev. B* **2005**, *71*, 235101.
55. Kohn, W.; Sham, L. J. Self-Consistent Equations Including Exchange and Correlation Effects. *Phys. Rev.* **1965**, *140*, A1133–A1138.
56. Basanta, M. A.; Dappe, Y. J.; Jelínek, P.; Ortega, J. Optimized Atomic-like Orbitals for First-Principles Tight-Binding Molecular Dynamics. *Comput. Mater. Sci.* **2007**, *39*, 759–766.
57. Sugimoto, Y.; Pou, P.; Custance, O.; Jelínek, P.; Abe, M.; Pérez, R.; Morita, S. Complex Patterning by Vertical Interchange Atom Manipulation Using Atomic Force Microscopy. *Science* **2008**, *322*, 413–417.